MOL #75341

Heteromeric TRPC1/TRPC4 channels play a critical role in epileptiform burst firing and seizure-induced neurodegeneration

Kevin D. Phelan, Matthew M. Mock, Oliver Kretz, U Thaung Shwe, Maxim Kozhemyakin, L. John Greenfield, Alexander Dietrich, Lutz Birnbaumer, Marc Freichel, Veit Flockerzi and Fang Zheng

Department of Neurobiology and Developmental Sciences, University of Arkansas for Medical Sciences, Little Rock, AR 72205 (KDP)

Department of Pharmacology and Toxicology, University of Arkansas for Medical Sciences, Little Rock, AR 72205 (MMM, UTS, FZ)

Department of Neurology, University of Arkansas for Medical Sciences, Little Rock, AR 72205 (MK, LJG)

Institute of Anatomy and Cell Biology, University of Freiburg, D-79104 Freiburg, Germany (OK)

LM-University Munich, Walther-Straub-Institute for Pharmacology and Toxicology, Nussbaumstr. 26, 80336 Munich, Germany (AD)

National Institute of Environmental Health Sciences, 111 TW Alexander Dr., Research Triangle Park, North Carolina 27709 (LB)

Experimentelle und Klinische Pharmakologie und Toxikologie, Gebäude 46, Medizinische Fakultät, Universität des Saarlandes, 66421 Homburg, Germany (MF, VF)

MOL #75341

Running Title: TRPC channels, epileptiform burst firing and neurodegeneration

Corresponding author:

Fang Zheng, Ph.D.,

Associate Professor,

Department of Pharmacology and Toxicology,

University of Arkansas for Medical Sciences, Little Rock, AR 72205.

Email: zhengfang@uams.edu

30 Pages

6 Figures

29 References

Abstract: 205 words

Introduction: 431 words

Discussion: 687 words

Abbreviations: Canonical transient receptor channels (TRPC); metabotropic glutamate receptors (mGluRs); Fluoro-Jade C (FJC); (1S,3R)-1-Aminocyclopentane-1,3-dicarboxylic acid (1S,3R-ACPD); (S)-3,5-dihydroxyphenyl-glycine (DHPG); (2R,4R)-4-Aminopyrrolidine-2,4-dicarboxylate (APDC); (RS)-4-Phosphonophenylglycine (PPG); (S)-(+)-α-Amino-4-carboxy-2-methylbenzeneacetic acid (LY367385); 7-(Hydroxyimino)cyclopropa[b]chromen-1a-carboxylate ethyl ester (CPCCOEt); 1-[2-(4-Methoxyphenyl)-2-[3-(4-methoxyphenyl)propoxy]ethyl-1H-imidazole (SKF96365); dorsolateral septal nucleus (DLSN); *Status Epilepticus* (SE)

MOL #75341

Abstract

Canonical transient receptor channels (TRPCs) are receptor-operated cation channels which are activated in response to phospholipase C signaling. Although TRPC1 is ubiquitously expressed in the brain, TRPC4 expression is the most restrictive, with the highest expression level limited to the lateral septum. The subunit composition of neuronal TRPC channels remains uncertain because of conflicting data from recombinant expression systems. Here we report that the large depolarizing plateau potential that underlies the epileptiform burst firing induced by metabotropic glutamate receptor agonists in lateral septal neurons was completely abolished in TRPC1/4 double knockout mice, and was abolished in 74% of lateral septal neurons in TRPC1 knockout mice. Furthermore, neuronal cell death in the lateral septum and the CA1 region of hippocampus after pilocarpine-induced severe seizures was significantly ameliorated in TRPC1/4 double knockout mice. Our data suggest that both TRPC1 and TRPC4 are essential for an intrinsic membrane conductance mediating the plateau potential in lateral septal neurons, possibly as heteromeric channels. Moreover, excitotoxic neuronal cell death, an underlying process for many neurological diseases, is not merely mediated by ionotropic glutamate receptors, but also by heteromeric TRPC channels activated by metabotropic glutamate receptors. TRPC channels could be an unsuspected but critical molecular target for clinical intervention for excitotoxicity.

Introduction

Canonical transient receptor channels (TRPCs) are mammalian homologues of the *Drosophila* transient receptor potential channel gene (Birnbaumer et al., 2003; Pedersen et al, 2005), and are thought to be receptor-operated cation channels activated in response to phospholipase C-coupled receptors and signaling (Desai et al., 2005; Venkatachalam and Montell, 2007). Although several TRPCs are highly expressed in the brain (Zhu et al., 1996; Philipp et al, 1996), their functional roles remain controversial. An earlier report suggested that TRPC1 channels coupled to mGluR1 mediate the slow synaptic responses in cerebellar Purkinje neurons (Kim et al., 2003). However, a recent study using TRPC knockout mice indicates that TRPC3, not TRPC1, underlies this synaptic response (Hartmann et al., 2008). Among the 7 members of the TRPC family, TRPC1 transcripts are ubiquitously expressed in the brain, and moderate to high expression of TRPC1 can be detected in most limbic areas (Zhu et al., 1996; Lein et al., 2007). On the other hand, transcripts of the remaining members of the TRPC family have a more discrete expression pattern in the brain, and TRPC4 has the most restricted pattern of expression, as noted by the highest expression in the lateral septum (Lein et al., 2007, Mori et al., 1998). Given its unique expression pattern of TRPC channels, the lateral septum offers an ideal brain area for the study of functional roles of neuronal TRPC channels.

The lateral septum is also noted for its high vulnerability to seizure-induced neuronal cell death as well as direct excitotoxicity induced by selective agonists for metabotropic glutamate receptors (mGluRs) (McDonald et al., 1993). Activation of group I mGluRs, i.e. mGluR1 and mGluR5, leads to membrane depolarization and spontaneous burst firing with a prominent plateau potential in rat lateral septal neurons (Zheng and Gallagher, 1991; Zheng and Gallagher, 1995). This plateau potential corresponds to an inward current under voltage-clamp, permeable to both sodium and

4

calcium, with a negative slope region in the current-voltage (I-V) relationship (Zheng et al., 1995; Raggenbass et al., 1997). This plateau potential induced by mGluR agonists may be mediated by heteromeric TRPC channels comprised of TRPC1 and TRPC4. To test this hypothesis, we explored the functional roles of TRPC channels with a panel of single and double knockouts of various TRPC family members. We found that both TRPC1 and TRPC4 are required for this plateau potential. Furthermore, the neurodegeneration observed after pilocarpine-induced seizure is greatly reduced in both the lateral septum and hippocampus in TRPC1/4 double knockout mice. Our data support the notion that TRPC channels, in particular heteromeric TRPC1/4 channels, are involved in epileptiform burst firing and excitotoxicity.

Materials and Methods

Electrophysiological recordings. Transverse slices of adult mouse forebrain containing the septal nucleus were obtained from approximately 2 month old wild-type (F1 50:50, C57BL6:129SvJ), TRPC1, 3, 5 or 6 knockout and TRPC1/4 double knockout mice. The mice were anesthetized with ketamine (60 mg/kg, I.M.) followed by decapitation. The brain was quickly removed from the skull and briefly immersed in a modified ice-cold artificial cerebrospinal fluid (ACSF) (Zheng et al., 1996) that was bubbled continuously with 95% O_2 and 5% CO_2 to maintain pH at 7.3 to 7.4. Serial 500 μm thick sections were cut with a Vibraslice and allowed to recover in oxygenated ACSF for at least one hour at room temperature prior to recording. A single septal slice was held submerged in the recording chamber between two nylon meshes and superfused with oxygenated ACSF warmed to 32º±1ºC at a rate of 1-2 ml/min. Microelectrodes were pulled from filamented borosilicate glass on a Flaming Brown Micropipette Puller (Model P-97) to a final tip resistance of 60 to 90 MΩ when filled with 3M potassium acetate. Voltage signals were recorded in the current-clamp mode with an Axoclamp

2B amplifier (Axon Instruments) and digitized using a model 1322A Digidata interface and pClamp 9 or pClamp 10 (Axon Instruments) and stored on a computer hard drive. Whole cell patch clamp recording was conducted under visual guidance in 300 μm thick coronal slices at the room temperature with an Axopatch 700 amplifier and the data were collected with pClamp 10. The internal solution for patch pipettes (with tip resistances between 5-8 MΩ) contained the following (in mM): 110 Cs-gluconate, 30 CsCl, 2 $MgCl_2$, 4 NaCl, 0.5 $CaCl_2$, 5 Cs-BAPTA, 10 HEPES, 2 NaATP, 0.3 NaGTP (pH 7.3).

Quantitative real-time PCR. Septal nuclei and hippocampi were dissected from wildtype mice and total RNA was isolated using the Qiagen RNA spin column according to the manufacturer's instructions, and treated with DNase, then reverse transcribed (iScript cDNA, Biorad) to generate cDNA. Target cDNA sequences were amplified by PCR using iQ SYBR Green Supermix (Biorad). After initial denaturation at 95°C for 3 min, the temperature-cycling profile for amplification was (40 cycles): 95°C for 10 s denaturing and 62°C for 1 min for annealing and extension, followed by a melting curve analysis accomplished in 80 cycles. Data were analyzed using iCycler software (Biorad). The primers used for RT-PCR were as described previously (Dietrich et al., 2005).

Antibodies. The polyclonal anti-TRPC4 antisera 781 was generated in-house and was preabsorbed before use to microsomal membrane protein fractions obtained from brain of TRPC4 knockout mice.

Electron microscopy. Adult mice were anesthetized with sodium pentobarbital and transcardiacally perfused with 4% paraformaldehyde and 0.1% glutaraldehyde in 0.1 M phosphate buffer (PB). The brains were removed and postfixed in the same fixative (overnight at 4°C) and then washed in phosphate buffered saline (PBS). Transverse sections (50 μm) were cut

6

on a vibratome and cryoprotected in a solution containing 25% sucrose and 10% glycerol in 50 mM PBS. The sections were freeze-thawed and incubated in blocking solution containing 2% normal goat serum in 50 mM Tris-buffered saline for 1 hour, followed by incubation with the anti-TRPC4 antiserum 781 (1:50 for 48 hours at 4°C). Negative controls consisted of using the same staining procedure in TRPC4 knockout mice brain as well as staining wildtype slices without primary antibody incubation. After the sections were washed, they were incubated with 1.4-nm gold-coupled goat anti-rabbit secondary antibody (1:100, Nanogold; Nanoprobes, Stony Brook, NY) for immunogold reaction. Immunogold labelling was then enhanced with HQ silver kit (Nanoprobes). After treatment with OsO4, the sections were stained with uranyl acetate, dehydrated, and flat-embedded in epoxy resin (Durcupan ACM, Fluka; Sigma-Aldrich, Gillingham, UK). Ultrathin sections were cut and then analyzed using a Philips CM 100 electron microscope.

Immunohistochemistry. After the brain was removed, transverse sections of 50 µm thickness were cut using a vibratome. Sections were washed in 0.1 M PB and then incubated overnight at 4°C using antibody 781 at 1:100 dilution. After washing in 0.1 M PB, sections were incubated in secondary antibodies coupled to cy2 or cy3 (1:100, Dianova, Hamburg, Germany) overnight at 4°C. After the sections were rinsed in 0.1 M PB for 1 hour, they were coverslipped with Vectastain mounting media (Vector Laboratories). Immunofluorescent double labelling was performed by sequential incubation with anti-TRPC4 antibody 781 and antibody for NeuN (1:100, Millipore, Billerica, MA), or mGluR1 (1:1000, Chemicon, Temecula, CA) or syntaxin (1:1000, Synaptic Systems, Göttingen, Germany), respectively.

Pilocarpine-induced seizure. Age-matched wildtype or TRPC1/4 double knockout mice (2-6 months old) were injected with a single dose of pilocarpine (i.p.) at one of the following dosages:

175, 222, 280 mg/kg 30 min after an injection of methylscopolamine nitrate (1mg/kg; i.p.) to block the peripheral effects of pilocarpine. Seizures induced by pilocarpine were recorded by a digital camcorder and scored at a later time for each 5-min period. The scoring was based on the modified Racine scale, as described at the following stages: 0, no abnormality; 1, exploring, sniffing, and grooming ceased, becoming motionless; 2, forelimb and/or tail extension, appearance of rigid posture; 3, myoclonic jerks of the head and neck, with brief twitching movement, or repetitive movements with head bobbing; 4, forelimb clonus and partial rearing, or occasional rearing and falling; 5, forelimb clonus, continuous rearing and falling; 6, tonic-clonic movements with loss of posture tone, often resulting in death. Mice were allowed to survive for 2 days and perfused to assess the seizure-induced neurodegeneration. Fluoro-Jade C (FJC) staining was performed on selected sections from all WT mice. Only 1 of 12 WT mice with an average seizure score of 3 and below was positive for FJC staining while all 9 WT mice with an average seizure score of above 3 were positive for FJC staining. Therefore, our modified Racine scale provided a good predictor for the likelihood of pilocarpine-induced neuronal cell death.

Screening for neurodegeneration with Fluoro-Jade C staining. Two days after pilocarpine-induced seizures, mice were anesthetized with ketamine (60 mg/kg, I.M.) and then intracardiacally perfused using a peristaltic pump. A brief heparinized phosphate buffered saline rinse was followed by a 4% paraformaldehyde fixative in 0.1 M phosphate buffer. The brains were removed from the skull, postfixed for at least 48 hrs, cut into a transverse block of tissue containing the hippocampus and septum, and glued to the cutting stage of a Vibratome (Pelco 1500, Ted Pella Inc.). Serial coronal sections were cut at 50 μm thickness and collected in 0.1 M phosphate buffer in a 24 well plate and stored at 4°C. Free-floating sections were stained with FJC as reported previously (Schmued et al., 2005). Two sections at least 300 μm apart from

septal and hippocampal regions were processed for spot check. If FJC positive neurons were found, a complete series of 150 μm spaced sections were further stained with FJC. Images of FJC-positive sections were captured using a Coolsnap fx camera (Photometrics) mounted on an Olympus fluorescent microscope.

Nissl counterstaining and analysis of cell death. Coronal sections (50 μm thick) was stained with 0.1% cresyl violet solution. Unbiased cell counting was obtained using Stereologer (Stereology Resource Center) to project a systematic grid of dissector frames onto the hippocampus in serial Nissl stained sections spaced 150 μm apart extending from stereotaxic coordinates of bregma -1.3 to -2.3 mm. The pyramidal cell layer was divided into the "CA1" section (including both the CA1 and the CA2) and the "CA3" section. The hilar region was defined as the area outlined by the densely packed granule cell layer and a straight line drawn between the two tips of the granule cell layer. The size of the dissectors and spacing were: 500, 600 and 900 μm^2 and 100, 75 and 100 μm apart for the CA1, the CA3 and the hilar regions respectively. Only those cells displaying Nissl stained cytoplasm with a nucleus whose top was completely within the section were counted. Cells were included if they fell partly or wholly within the dissector frame and did not cross the exclusion lines. The total number of cells (N) was estimated using the formula "N = n * 1/ASF * 1/SSF * 1/TSF" where n is the number of cells counted, ASF is the area sampling fraction, SSF is the section sampling fraction and TSF is the tissue sampling fraction. Due to the small number of surviving neurons remaining in these hippocampal regions after pilocarpine-induced seizures, we used the maximal size of the dissector in the z axis (i.e., the tissue sampling fraction was 1). The coefficients of error (CEs) for all three regions in both groups were acceptable (ranging from 0.07 to 0.17).

Results

TRPC1 and TRPC4 are the main TRPCs expressed in the septum and hippocampus

We used the real-time PCR method to determine the relative level of expression of each TRPC in the septum compared to the hippocampus (Figure 1A). We found that TRPC1 and TRPC4 are highly expressed in the septal area, followed by TRPC3 at approximately 10 fold lower levels, whereas the expression of other TRPCs is at least 50 fold lower than that of TRPC1 and TRPC4. TRPC1 and TRPC4 were also the most prominent TRPCs expressed in the hippocampus (Figure 1A). To determine whether the expression of TPRC4 is neuronal, brain sections were stained with an in-house generated anti-TRPC4 antibody (Fig.1B). As shown in Figure 1C, the anti-TRPC4 antibody produced wide spread immunoreactivity in lateral septal neurons, which is absent in the TRPC4 knockout mice (Figure 1D). Double labeling with a neuronal marker (NeuN) confirmed the presence of TRPC4 in the soma and primary dendrites of lateral septal neurons (Figure 1E). Furthermore, immunogold labelling showed that within lateral septal neurons, TRPC4 was localized predominantly at the plasma membrane of the soma and proximal dendrites (Figure 1F-G). Occasionally, immunogold labelling was detected at the rough endoplasmic reticulum. In contrast, axons and presynaptic profiles did not show TRPC4 immunogold labelling. Double labeling with anti-TRPC4 and anti-mGluR1 antibodies showed co-localization of TRPC4 and mGluR1 in lateral septal neurons (Figure 1H). Hippocampal neurons also exhibited intense TRPC4 staining that was largely not overlapping with syntaxin staining (Figure 1I). Taken together, our data suggest that TRPC1 and TRPC4 are likely the predominant neuronal TRPC channels in the lateral septum and the hippocampus.

Both TRPC1 and TRPC4 are required for the plateau potential induced by activation of group I mGluRs in the lateral septum

Given the expression level of TRPC1 and TRPC4 in the lateral septum, the plateau potential that underlies the epileptiform burst firing induced by mGluR agonists reported previously (Zheng and Gallagher, 1991; Zheng and Gallagher, 1995) may be mediated by heteromeric TRPC channels comprised of TRPC1 and TRPC4. As in rat lateral septal neurons, the mGluR agonist (1S,3R)-1-Aminocyclopentane-1,3-dicarboxylic acid (1S,3R-ACPD) induced epileptiform burst firings with an underlying plateau potential. Without 1S,3R-ACPD, injection of a series of current step pulses (20 ms, 0.1-1.0 nA, -80 mV) was followed by a simple decay of the membrane potential back towards baseline (Figure 2A; n=13). In the presence of 30 μM 1S,3R-ACPD (n=13), a short-duration prominent subthreshold depolarizing response first appeared as injection of current increased (open arrowhead), followed by the appearance of a prolonged plateau depolarizing response at the higher intensity of current steps (arrow) (Figure 2A). In addition to 1S,3R-ACPD, (S)-3,5-dihydroxyphenyl-glycine (DHPG), a group 1 selective agonist, also induced a plateau potential at 30-100 μM (n=8, data not shown). On the other hand, the group II select agonist (2R,4R)-4-Aminopyrrolidine-2,4-dicarboxylate (APDC; 20 μM) and the group III selective agonist (RS)-4-Phosphonophenylglycine (PPG; 100 μM) were unable to induce a plateau potential in lateral septal neurons (n=6 and 3, respectively; data not shown). Furthermore, the plateau potential induced by 1S,3R-ACPD in lateral septal neurons was abolished by (S)-(+)-α-Amino-4-carboxy-2-methyl-benzeneacetic acid (LY367385; 100 μM) and 7-(Hydroxyimino)cyclopropa[b]chromen-1a-carboxylate ethyl ester (CPCCOEt; 10 μM) (Fig.2B). Taken together, our data strongly suggest that the plateau potential underlying the epileptiform burst firing induced by 1S, 3R-ACPD in lateral septal neurons was mediated by group I mGluRs.

MOL #75341

To test whether the plateau potential that underlies epileptiform burst firing induced by 1S,3R-ACPD in lateral septal neurons was mediated by TRPC channels, we first tested the effect of 1-[2-(4-Methoxyphenyl)-2-[3-(4-methoxyphenyl)propoxy]ethyl-1H-imidazole (SKF96365), which is frequently used as a TRPC channel blocker (Kim et al., 2003; Gee et al, 2003). Superfusion of SKF96365 (20 µM) resulted in a complete block of the 1S,3R-ACPD-induced subthreshold and plateau depolarizing responses (Figure 3A; n=3). However, SKF96365 may exert a number of additional effects on cell signaling (Putney, 2005), and we therefore sought confirmation of the role of TRPC channels using TRPC knockout mice. TRPC1 (Dietrich et al., 2007) and TRPC4 knockout mice (Freichel et al., 2001) were crossbred to obtain the double knockout of TRPC1 and TRPC4. In TRPC1/4 double knockout mice, the plateau potential was completely absent in the lateral septal neurons (n=10) (Figure 3B, C). Thus, both TRPC1 and TRPC4 are required for the full plateau potential induced by mGluR agonists in lateral septal neurons. We further examined the individual role of TRPC1 and TRPC4. A majority of lateral septal neurons in TRPC1 knockout mice (approximately 74%, 20 of 27 cells) lacked 1S,3R-ACPD-induced full plateau potentials (Figure 3C), while the plateau potential remained in some lateral septal neurons (26%, 7 of 27 cells; Figure 3C). We recorded from TRPC4 knockout rats (Transposagen, Lexington, KY) and found that all lateral septal neurons recorded (n=10) lacked the ACPD-induced burst firing and plateau potential (data not shown). Thus, data from TRPC1 and TRPC4 single knockout animals were consistent with the data from TRPC1/4 double knockout mice, confirming that both TRPC1 and TRPC4 are critical for the plateau potential induced by 1S,3R-ACPD in lateral septal neurons. In contrast to TRPC1 and TRPC4 knockout, normal plateau potentials induced by 1S,3R-ACPD in lateral septal neurons were observed in TRPC3 (12 out of 13) and TRPC5 (8 out of 9) and TRPC6 (8 out of 8) knockout mice,

suggesting that these members of the TRPC family play a minimal role in the mGluR1/5 mediated plateau potential. Our data suggest that the plateau potential is mediated primarily by heteromeric TRPC1/4 channels. The plateau potential seen in a small group of lateral septal neurons in TRPC1 knockout mice is likely mediated by either homomeric TRPC4 channels or heteromeric TRPC channels comprised of TRPC4 and other unidentified members. However, such TRPC channels are insufficient for mediating the plateau potential in the majority of lateral septal neurons. Furthermore, the pattern of spontaneous firing in the presence of 1S-3R-ACPD was also different in the wildtype and TRPC1/4 double knockout mice (Figure 3B). In the wildtype mice, 1S,3R-ACPD induced spontaneous burst firing, and each burst consisted of several action potentials and lasted several hundreds of milliseconds. Such spontaneous burst firing was also absent in TRPC1/4 double knockout mice. Under voltage clamp, the current induced by 1S,3R-ACPD in WT lateral septal neurons in the presence of blockers for voltage-gated sodium and calcium channels exhibited an I-V relationship characterized by a large inward current with a very prominent negative slope region and a reversal potential near +20 mV (Figure 3D, the left panel). The addition of 20 μM SKF96365 to 1S,3R-ACPD in the bath solution significantly reduced the inward current with the negative slope region and shifted the reversal potential to a more negative range (n=3). In TRPC1/4 double knockout mice (n=4), we did not observe the typical significant inward current with a prominent negative slope region, although there was a small inward current at more depolarized membrane potentials (more positive than -40 mV) that was sensitive to SKF96365 (20 μM) (Figure 3D, the right panel). Taken together, our data suggest that heteromeric TRPC1/4 channels in lateral septal neurons play a critical role in metabotropic glutamate receptor-mediated modulation of the firing pattern of these neurons.

Seizure-induced neuronal cell death is greatly reduced in TRPC1/4 double knockout

Lateral septal neurons exhibit mGluR agonist-induced neuronal cell death, and the plateau potential underlying the epileptiform burst firing, which allows a huge calcium influx into these neurons, has been suggested as the potential underlying mechanism (Zheng et al., 1996). If there is a link between the plateau potential and the neuronal cell death, the TRPC1/4 double knockout mice that completely lack the plateau potential should exhibit reduced excitotoxic neuronal cell death in the lateral septum. To test if this is the case, we adopted the well-established pilocarpine-induced *Status Epilepticus* (SE) model (Cavalheiro et a., 1996; Borges et al., 2003) that leads to extensive neuronal cell death in the lateral septum. Wildtype and TRPC1/4 double knockout mice were treated with a single dose of pilocarpine (175 or 280 mg/kg, i.p.) and the resulting seizures were videotaped and scored for 90 minutes or 180 minutes if grade 3 or above persisted after 90 minutes. The average seizure score during the period between 20-90 minutes after the pilocarpine injection for wildtype and TRPC1/4 double knockout mice were shown in Figure 4A. Statistical analysis showed that there was no significant differences between the wildtype and TRPC1/4 double knockout mice (Two-way ANOVA, $p > 0.05$). Thus, the TRPC1/4 double knockout mice appear to show normal sensitivity to pilocarpine. However, the mortality rate after pilocarpine treatment was significantly reduced in the TRPC1/4 double knockout mice. For wildtype mice, the mortality rate exhibited a dose dependency, with a comparable high mortality rate at the 222 and 280 mg/kg dosages (Figure 4B). For TRPC1/4 double knockout mice, the mortality rate was 0% at the 175 and 280 mg/kg dosages. Since there were no wildtype survivors with severe seizures (stage 4 and above) after 280 mg/kg pilocarpine injection, we compared the seizure-induced neuronal cell death using Fluoro-Jade C (FJC) staining in a group of wildtype mice treated with 175 mg/kg pilocarpine to a group of TRPC1/4 double knockout

mice treated with 280 mg/kg pilocarpine with comparable average seizure scores (Figure 4D, left panel). Figure 4C shows the representative neuronal cell death in the dorsolateral septal nucleus (DLSN) in the wildtype and TRPC1/4 double knockout mice. As expected, the neuronal cell death resulting from pilocarpine-induced SE in the DLSN was significantly reduced in the TRPC1/4 double knockout mice (Figure 4D, right panel). Our data suggest that TRPC1 and TRPC4 play a critical role in excitotoxicity in the DLSN.

Surprisingly, the reduction of seizure-induced neurodegeneration was not limited to the DLSN. There appeared to be widespread decreases in seizure-induced neurodegeneration in the limbic system. The hippocampus is one of the most vulnerable brain structures to seizures and extensive neurodegeneration typically occurs after pilocarpine treatment in the CA1 and CA3 subfields (Borges et al., 2003). Neurodegeneration after pilocarpine-induced seizures in the hippocampus was first examined using FJC stained sections. Two days after pilocarpine-induced SE, most wildtype mice exhibited consistent severe loss of CA3 and CA1 pyramidal neurons (Figure 5A), although the extent of CA1 degeneration showed some variability. The neurodegeneration indicated by histological observations (shown in Figure 5C, E and F) in wildtype mice generally correlates with FJC staining (Figure 5A). In most wildtype mice, only a few pyramidal neuron cell bodies remained intact in the CA1 and CA3 regions, accompanied by severe gliosis. In TRPC1/4 double knockout mice, there were only scattered FJC-positive neurons in the CA1 region and the density of FJC positive neurons in the CA3 region was also clearly reduced (Figure 5B). Nissl-stained sections from TRPC1/4 double knockout mice showed that, after pilocarpine-induced seizures, the pyramidal cell layer in the CA3 and CA1 regions remained intact, and a majority of mice showed no significant gliosis (Figure 5 D, G and H). The total estimated numbers of surviving neurons in the CA1/CA2, the CA3 and the hilar

regions of hippocampus were determined using Stereologer from these Nissl stained sections

(Figure 6). TRPC1/4 double knockout mice showed more surviving neurons in all three regions,

although only the increase in CA1/CA2 region was statistically significant. The lack of

statistical significance in the CA3 between WT and TRPC1/4 double knockout mice was due to

the fact that the neuronal cell death after pilocarpine-induced seizure is concentrated in the b/c

subfield of CA3 (Figure 5C, solid arrows). However, we were not able to analyze these

subfields with stereological methods because there was no objective boundary for them. We

then determined the extent of cell death in the CA3 regions of the hippocampus using a

qualitative approach as described previously (Borges et al., 2003): 0, no detectable cell death; 1,

<25% cell death; 2, 25-49% cell death; 3, 50-74% cell death; 4, 75% or more. We found that the

neurodegeneration resulted from pilocarpine-induced seizures in the CA3 region was 3.75 ± 0.11

in the WT mice (n=5) and 0.85 ± 0.57 in the TRPC1/4 double knockout mice (n=5), which was

significantly different ($p<0.01$, Mann-Whitney test). Taken together, our data showed that

seizure-induced neurodegeneration was significantly reduced in the hippocampus. The observed

sparing of neuronal cell death in limbic regions in addition to the lateral septum in the TRPC1/4

double knockout mice implicates TRPC1 and TRPC4 as playing a more widespread role in

seizure-induced neuronal cell death in the CNS.

Discussion

In summary, our data suggest that heteromeric TRPC1/4 channels play novel roles in adult

brain in contrast to reported neurotrophic roles for TRPC3 and TRPC6 (Sossin and Barker,

2007). Lateral septal neurons express high levels of TRPC1 and 4 and only moderate to low

levels of other TRPCs. Taking advantage of a panel of TRPC single and double knockout mice,

we have now shown that heteromeric TRPC1/TRPC4 channels mediate the plateau potential

underlying mGluR agonist-induced epileptic burst firing in most lateral septal neurons. Although TRPC4 is absolutely required, a small percentage of lateral septal neurons in TRPC1 knockout exhibited full plateau potentials induced by mGluR agonists, raising some interesting questions about signaling leading up to the activation of TRPC channels in lateral septal neurons. Since our immunohistochemical staining indicated that most lateral septal neurons express TRPC4. homomeric TRPC4 channels could exist in these neurons. The lack of full plateau potentials induced by mGluR agonists in the majority of lateral septal neurons in TRPC1 knockout mice suggests that the coupling between mGluRs and homomeric TRPC4 channels is not sufficient for full activation. The presence of TRPC1 seems to be required for effective coupling between mGluR1/5 and TRPC channels. The lateral septal neurons clearly present an opportunity for more in-depth study of the activation and signal coupling of neuronal TRPC channels.

Our data also indicate a significant role of TRPC1/4 channels in seizure-induced neuronal cell death in both lateral septum and hippocampus. One likely scenario to explain how TRPC channels play a role in excitotoxicity in the limbic system is as follows: Under pathologic conditions, an excessive amount of glutamate is released, leading to activation of group I mGluRs (mGluR1 and 5). Activation of group I mGluRs, through a complex signaling network, increases the activation of TRPC channels that are likely heteromeric TRPC1/4 channels in lateral septal neurons. TRPC1/4 channels are further activated during neuronal firing and lead to a self-regenerative afterdepolarization (i.e. the plateau potential) that underlies the epileptiform discharges observed in the lateral septum. While TRPC1/4 channels were clearly required for the plateau potential, it is possible that other voltage gated channels, such as voltage-gated calcium channels may also participate in the plateau potential. Calcium overloading generated by the

mGluR-mediated plateau potential (Zheng et al., 1996) then leads to excitotoxicity. This scenario is supported by our present data: 1) the plateau potential is absent in TRPC1/4 double knockout mice; and 2) the SE-induced excitotoxicity in the lateral septum is reduced in TRPC1/4 double knockout mice. The exact functional role of TRPC1/4 channels in lateral septal neurons under physiological conditions is not clear yet, and needs to be elucidated with additional work using the panel of various TRPC KO mice. One possibility is that TRPC1/4 channels may be involved in the generation of theta rhythm in the limbic system.

The precise mechanism by which TRPC1/4 channels contribute to seizure-induced excitotoxicity in other limbic regions remains to be determined. Under normal conditions, hippocampal pyramidal cells lack the kind of self-regenerative plateau potentials induced by mGluR agonists in the lateral septum, although an mGluR-mediated TRPC-like inward current has been reported (Gee et al., 2003). Furthermore, it has been reported that activation of group I mGluR leads to altered surface expression of TRPC channels (Wang et al., 2007). It is possible that TRPC channels may mediate membrane depolarization and/or calcium influx in hippocampal neurons during the pilocarpine-induced seizure and therefore contribute to excitotoxicity.

Excitotoxicity plays a central role in the pathophysiology of epilepsy, stroke and head trauma (Choi, 1988; Lipton and Rosenberg, 1994; Olney, 2003). It has been assumed for years that the excitotoxicity is mainly mediated by NMDA receptors with a contribution from voltage-gated calcium channels (Choi, 1988; Lipton and Rosenberg, 1994; Olney, 2003). Our data reveals that TRPC1/4 channels are new critical players in excitotoxicity not only in the lateral septum, but also in the hippocampus. Furthermore, a preliminary analysis shows widespread sparing of forebrain neurons from seizure-induced cell death. TRPC channels should be considered as a

MOL #75341

promising novel target for developing new drug treatment for a wide variety of neurological

diseases in which excitotoxicity plays a role.

MOL #75341

MOL #75341

Authorship Contributions:

Participated in research design: Zheng, Phelan, Flockerzi, Freichel, Birnbaumer

Conducted experiments: Phelan, Zheng, Mock, Shwe, Kozhemyakin, Kretz, Flockerzi

Contributed new reagents or analytic tools: Dietrich, Freichel, Flockerzi, Birmbaumer

Performed data analysis: Zheng, Phelan, Shwe, Mock

Wrote or contributed to the writing of the manuscript: Zheng, Phelan, Greenfield, Birnbaumer,

Flockerzi, Freichel, Dietrich

REFERENCES

Birnbaumer L, Yildirim E, Abramowitz J (2003) A comparison of the genes coding for canonical TRP channels and their M, V and P relatives. *Cell Calcium* **33**: 419–432.

Borges K, Gearing M, McDermott DL, Smith AB, Almonte AG, Wainer BH, Dingledine R (2003) Neuronal and glial pathological changes during epileptogenesis in the mouse pilocarpine model. *Exp Neurol* **182**: 21-34.

Cavalheiro EA, Santos NF, Priel MR (1996) The pilocarpine model of epilepsy in mice. *Epilepsia* **37**: 1015-1019.

Choi DW (1988) Glutamate neurotoxicity and diseases of the nervous system. *Neuron* **1**: 623-634.

Desai BN, Clapham DE (2005) TRP channels and mice deficient in TRP channels. *Pflugers Arch – Eur J Physiol* **451**: 11–18.

Dietrich A, Kalwa H, Storch U, Mederos Y Schnitzler M, Salanova B, Pinkenburg O, Dubrovska G, Essin K, Gollasch M, Birnbaumer L, Gudermann T (2007) Pressure-induced and store-operated cation influx in vascular smooth muscle cells is independent of TRPC1. *Pflugers Arch* **455**: 465-477.

Dietrich A, Mederos Y Schnitzler M, Gollasch M, Gross V, Storch U, Dubrovska G, Obst M, Yildirim E, Salanova B, Kalwa H, Essin K, Pinkenburg O, Luft FC, Gudermann T, Birnbaumer L (2005) Increased vascular smooth muscle contractility in TRPC6-/- mice. *Mol Cell Biol* **25**: 6980-6989.

Freichel M, Suh SH, Pfeifer A, Schweig U, Trost C, Weissgerber P, Biel M, Philipp S, Freise D, Droogmans G, Hofmann F, Flockerzi V, Nilius B (2001) Lack of an endothelial store-

operated Ca^{2+} current impairs agonist-dependent vasorelaxation in TRP4-/- mice. *Nat Cell Biol* **3**: 121-127.

Gee CE, Benquet P, Gerber U (2003) Group I metabotropic glutamate receptors activate a calcium-sensitive transient receptor potential-like conductance in rat hippocampus. *J Physiol* **546**: 655-664.

Hartmann, J, Dragicevic E, Adelsberger H, Henning HA, Sumser M, Abramowitz J, Blum R, Dietrich A, Freichel M, Flockerzi V, Birnbaumer L, Konnerth A (2008) TRPC3 channels are required for synaptic transmission and motor coordination. *Neuron* **59**:392-398.

Kim SJ, Kim YS, Yuan JP, Petralia RS, Worley PF, Linden DJ (2003) Activation of TRPC1 cation channel by metabotropic glutamate receptor mGluR1. *Nature* **426**: 285-291

Lein, E.S., Hawrylycz, M.J. et. al. (2007) Genome-wide atlas of gene expression in the adult mouse brain. *Nature* **445**:168-176.

Lipton SA, Rosenberg PA (1994) Excitatory amino acids as a final common pathway in neurologic disorders. *N Engl J Med* **330**: 613–622.

McDonald JW, Fix AS, Tizzano JP, Schoepp DD (1993) Seizures and brain injury in neonatal rats induced by 1S, 3R-ACPD, a metabotropic glutamate receptor agonist. *J Neurosci* **13**: 4445-4455.

Mori Y, Takada N, Okada T, Wakamori M, Imoto K, Wanifuchi H, Oka H, Oba A, Ikenaka K, Kurosaki T (1998) Differential distribution of TRP Ca2+ channel isoforms in mouse brain. *Neuroreport* **9**: 507-515.

Olney JW (2003) Excitotoxicity, apoptosis and neuropsychiatric disorders. *Curr Opin Pharmacol* **3**:101-109.

Pedersen SF, Owsianik G, Nilius B (2005) TRP channels: an overview. *Cell Calcium* **38**: 233-252.

Philipp S, Cavalié A, Freichel M, Wissenbach U, Zimmer S, Trost C, Marquart A, Murakami M, Flockerzi V (1996) A mammalian capacitative calcium entry channel homologous to Drosophila TRP and TRPL. *EMBO J* **15**: 6166- 6171.

Putney J (2005) Physiological mechanisms of TRPC activation. *Pflugers Arch* **451**: 29-34.

Raggenbass M, Pierson P, Metzger D, Alberi S (1997) Action of a metabotropic glutamate receptor agonist in rat lateral septum: induction of a sodium-dependent inward aftercurrent. *Brain Res* **776**: 75-87.

Schmued LC, Stowers CC, Scallet AC, Xu L (2005) Fluoro-Jade C results in ultra high resolution and contrast labeling of degenerating neurons. *Brain Res* **1035**: 24-31.

Sossin WS, Barker PA (2007) Something old, something new: BDNF-induced neuron survival requires TRPC channel function. *Nature Neuroscience* **10**: 537-538.

Venkatachalam K, Montell C (2007) TRP Channels. *Annu Rev Biochem* **76**:387–417.

Wang M, Bianchi R, Chuang SC, Zhao W, Wong RK (2007) Group I metabotropic glutamate receptor-dependent TRPC channel trafficking in hippocampal neurons. *J Neurochem* **101**: 411-421.

Zheng F, Gallagher JP (1991) Trans-ACPD (trans-D,L-1-amino-1,3-cyclopentane-dicarboxylic acid) elicited oscillation of membrane potentials in rat dorsolateral septal nucleus neurons recorded intracellularly in vitro. *Neurosci Lett* **125**: 147-150.

Zheng F, Gallagher JP (1995) (1S,3R)-1-aminocyclopentane-1,3-dicarboxylic acid-induced burst firing is mediated by a native pertussis toxin-sensitive metabotropic receptor at rat dorsolateral septal nucleus neurons. *Neuroscience* **68**: 423-434.

Zheng F, Gallagher, JP, Connor JA (1996) Activation of a metabotropic glutamate receptor potentiates spike-driven calcium increases in neurons of the dorsolateral septum. *J Neurosci* **16**: 6079-6088.

Zheng F, Hasuo H, Gallagher JP (1995) 1S,3R-ACPD-prefering inward current in rat DLSN is mediated by a novel excitatory amino acid receptor. *Neuropharmacology* **34**: 905-917.

Zhu X, Jiang M, Peyton M, Boulay G, Hurst R, Stefani E, Birnbaumer L (1996) TRP, a novel mammalian gene family essential for agonist-activated capacitative Ca2+ entry. *Cell* **85**: 661-671.

MOL #75341

Footnote:

Figure Legends

Figure 1. TRPC1 and TRPC4 are the predominant TRPCs expressed in septum and hippocampus. **A:** Quantitative real-time PCR comparison of the relative expression of TRPCs in the septum and hippocampus of wildtype mice. The relative fold expression is plotted on a log scale as mRNA molecules per 1000 GAPDH mRNA molecules. **B:** Western blot analysis of TRPC4 expression in protein fractions obtained from brains of wild-type and TRPC4-knockout mice, respectively, with in-house generated anti-TRC4 antibody 781. In mouse tissues two variants of the TRPC4 protein are expressed, the "full-length" TRPC4 (TRPC4α) protein and a slightly smaller variant, called TRPC4Δ (or TRPC4β). **C-D:** Immunofluorescence labelling of TRPC4 in the septum of wildtype (C) and TRPC4 knockout mice (D). Scale bar: 300 μm (C and D), LS: Lateral septum; MS: Medial septum. **E**: Co-localization of TRPC4 (red) with the neuronal marker NeuN (green) in the lateral septum. Scale bars: 12 μm. **F-G:** Preembedding immunogold labelling for TRPC4 in the mouse lateral septum. Note that TRPC4 is predominantly localized at the post synaptic plasma membrane in close vicinity to the unlabelled presynaptic terminals. Scale bars: F: 0.5 μm, G: 0.2 μm. **H**: Co-localization of TRPC4 (red) and mGluR1 (green) in the septum. **I**: Colocalization of TRPC4 (red) and syntaxin (green) in the hippocampal CA3 region. Scale bars: H: 12 μm, I: 60 μm,.

Figure 2. Group I mGluRs mediate the plateau potentials induced by 1S,3R-ACPD in the

dorsolateral septum. **A**: In wildtype dorsolateral septal neurons, injection of a series of current

step pulses (20 ms, 0.1-1.0 nA, -80 mV) was followed by a simple decay of the membrane

potential. After superfusion of the group I mGluR agonist 1S,3R-ACPD (30 µM), injection of

the same series of current step pulses consistently induced the appearance of subthreshold (open

arrowhead) and prolonged plateau (arrow) depolarizing afterpotentials (n=13). Cells were

manually clamped at -80 mV to offset the agonist-induced membrane depolarization. B: Action

potentials were evoked by a brief depolarizing current step (0.8 nA, 20 ms) applied every 10

seconds. Superfusion of LY367385 (100 µM) resulted in a complete block of the 1S,3R-ACPD-

plateau depolarizing responses (left panel; 4 out of 4 lateral septal neurons). Similarly,

superfusion of CPCCOEt (10 µM) also blocked the 1S,3R-ACPD-induced plateau potential

(right panel; 4 out of 6 lateral septal neurons).

Figure 3. TRPC1 and TRPC4 mediate the plateau potentials underlying mGluR agonist-induced

epileptiform burst firing in the dorsolateral septum. **A**: Action potentials were evoked by a brief

depolarizing current step (0.8 nA, 20 ms) applied every 10 seconds. Superfusion of SKF96365

(20 µM) resulted in a complete block of the 1S,3R-ACPD-induced subthreshold and plateau

depolarizing responses (n=3) (red trace). The SKF96365 block was fully reversible upon

washout of the drug (blue trace). **B**: A brief depolarizing current step (0.8 nA, 20 ms) was

applied every 10 seconds to evoke action potentials , and 20 consecutive traces during the wash-

in of mGluR agonists were shown. Note the transition from normal firing to subthreshold

responses and the full plateaus as the agonist concentration increases during the wash-in.

Superfusion of 1S,3R-ACPD (30 µM) in TRPC1/4 double knockout (DKO) mice (n=10) failed

to induce the subthreshold or plateau depolarizing responses seen in age-matched wildtype

controls (i.e., 100% of the dorsolateral septal neurons in TRPC1/4 DKO mice were non-

responding cells). Consistent with the complete absence of mGluR agonist-induced plateau

responses, the dorsolateral septal neurons in TRPC1/4 DKO mice failed to exhibit the

spontaneous bursting seen in age-matched wildtype control cells after depolarizing the cells

during 1S,3R-ACPD superfusion by injecting a constant holding current (Inset, scale bar: 20mV,

500 ms). The input resistances of the dorsolateral septal neurons in the TRPC1/4 DKO mice

were not significantly different from that of wildtype neurons (78.5 $\pm$ 4.2 MΩ, and 68.5 $\pm$ 5.2

MΩ, respectively) (p>0.05, unpaired *t*-test). **C**: The percentage of cells exhibiting mGluR

agonist-induced full plateau potential in wildtype, TRPC1 knockout and TRPC1/4 DKO mice. **D**:

Neurons in the DLSN were recorded in whole-cell patch-clamp configuration (V_h, -65 mV). The

voltage-gated sodium and calcium channels were blocked by tetrodotoxin (1 μM) and Cd^{2+} (30

μM). The I-V relationship was then determined by a slow voltage ramp (-100 to +40 mV; 2

mV/sec). The current induced by 30 μM 1S,3R-ACPD (I-ACPD) or by 30 μM 1S,3R-ACPD

and 20 μM SKF96365 (I-ACPD,SKF) was determined by subtracting the control current from

the current in the presence of 1S,3R-ACPD or 30 μM 1S,3R-ACPD and 20 μM SKF96365.

Note the significant reduction of responses to 1S,3R-ACPD by SKF96365 in wildtype mice and

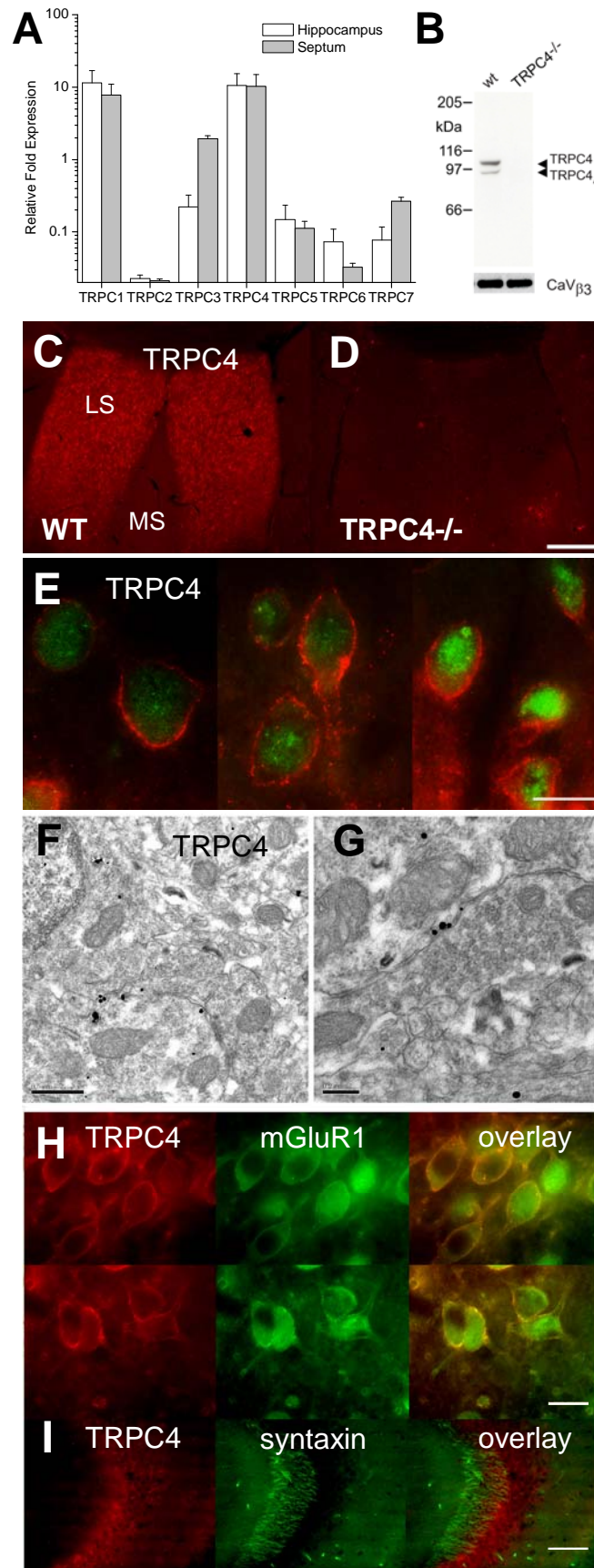the minimal response to 1S,3R-ACPD in TRPC1/4 DKO mice.

Figure 4. Seizure-induced neuronal cell death in the dorsolateral septum is significantly reduced in TRPC1/4 double knockout mice. **A**: Pilocarpine induces comparable intensities of seizures in wildtype and TRPC1/4 DKO mice (p>0.05, Two-way ANOVA). Pooled data (mean ± SEM) was plotted (n=24, 16 for WT at 175 and 280 mg/kg pilocarpine; n=12, 6 for TRPC1/4 DKO at 175 and 280mg/kg pilocarpine). See methods for description of seizure scale. **B**: The mortality following pilocarpine injections within the first 24 hours is significantly reduced in TRPC1/4 DKO mice (n=12, 6) compared to wildtype mice (n=24, 10, 16). **C**: Representative images of FJC stained neurons in the dorsolateral septal nucleus (DLSN) of wildtype and TRPC1/4 DKO mice (two day survival; wildtype: 175 mg/kg, TRPC1/4 DKO: 280 mg/kg). Scale Bar: 0.20 mm (0.05mm for the insets). **D**: Serial coronal sections containing septum (50 μm thick) were stained with FJC. FJC-positive neurons in the DLSN (see panel C) were counted in three sections approximately 300 μm apart. Mice (5 WT treated with 175 mg/kg pilocarpine; 5 TRPC1/4 DKO treated with 280 mg/kg pilocarpine) included in analysis showed comparable seizures. TRPC1/4 DKO mice exhibit a significant reduction in FJC-positive neurons in the DLSN (two-tailed unpaired *t*-test, **P<0.01).

Figure 5. Sparing of hippocampal neurons from pilocarpine seizure induced neurodegeneration in TRPC1/4 double knockout mice. **A-B**: Representative FJC stained transverse sections through the hippocampus in wildtype (A) and TRPC1/4 DKO (B) mice (two day survival; wildtype: 175 mg/kg, TRPC1/4 DKO: 280 mg/kg). **C-D**: Nissl staining in representative transverse sections through the hippocampus in wildtype (C) and TRPC1/4 DKO mice (D). There is a noticeable reduction of Nissl stained cell bodies in CA1 (open arrowhead) and CA3 (closed arrowhead) regions in wildtype but not TRPC1/4 DKO mice. **E-H**: High power photomicrographs illustrating the reduced gliosis and sparing of CA1 and CA3 neurons in the TRPC1/4 DKO hippocampus (G,H) versus the same regions in wildtype hippocampus (E,F). The photomicrographs were taken from regions demarcated by the arrowheads in C and comparable regions in D. Scale Bar: 200 μm (C-D); 50 μm (E-H).

Figure 6. Neuronal cell death after pilocarpine-induced seizure is reduced in TRPC1/4 double knockout mice. Serial coronal sections (50 μm) from mice with similar pilocarpine-induced seizures (see Fig.4D) were stained with Nissl and surviving neurons (with stained cytoplasm and round nuclei) were counted using Stereologer with a 100X oil-immersion objective. Note that number of the surviving neurons in the CA1 region is significantly higher in TRPC1/4 DKO mice ($p < 0.05$, two-tail unpaired t-test).
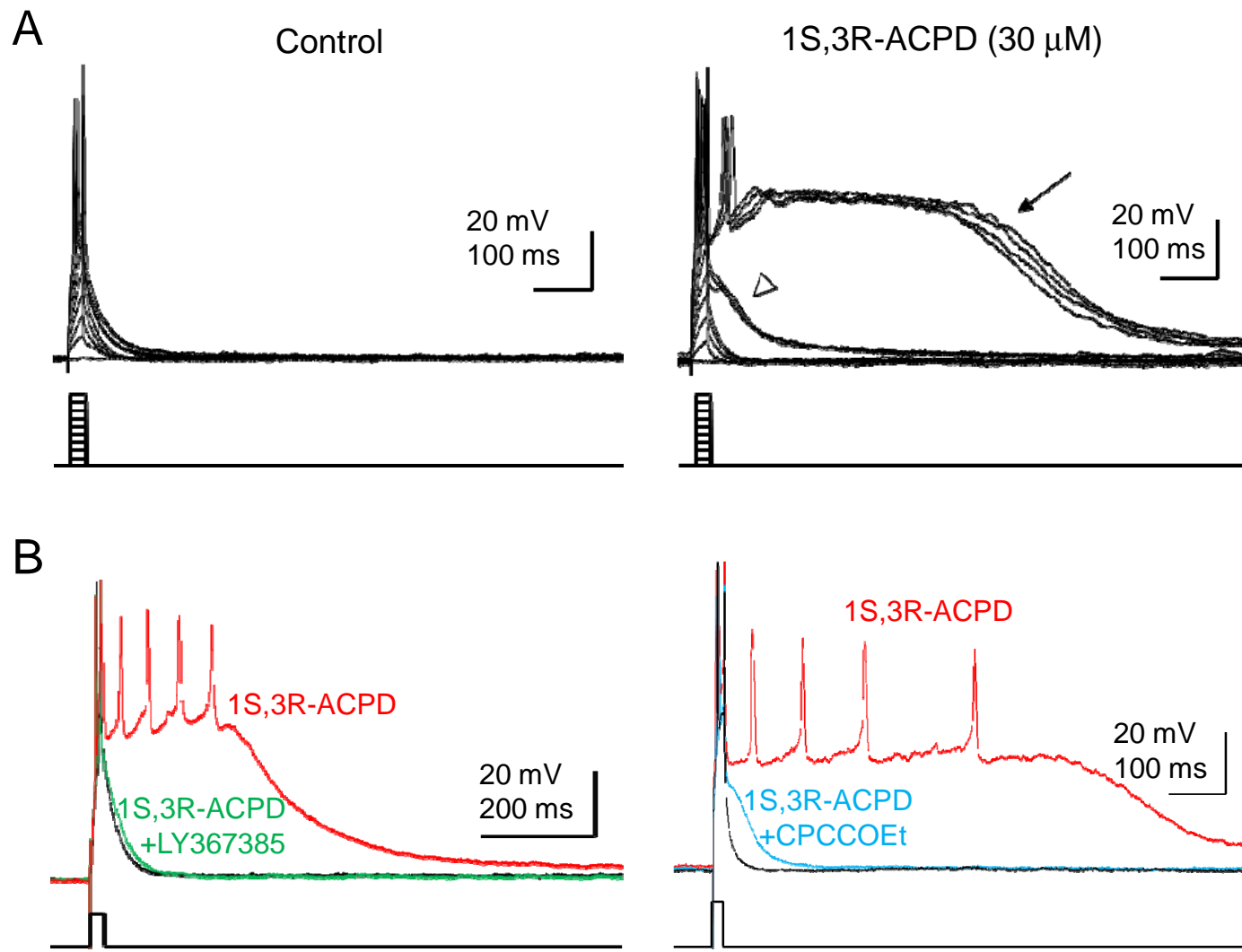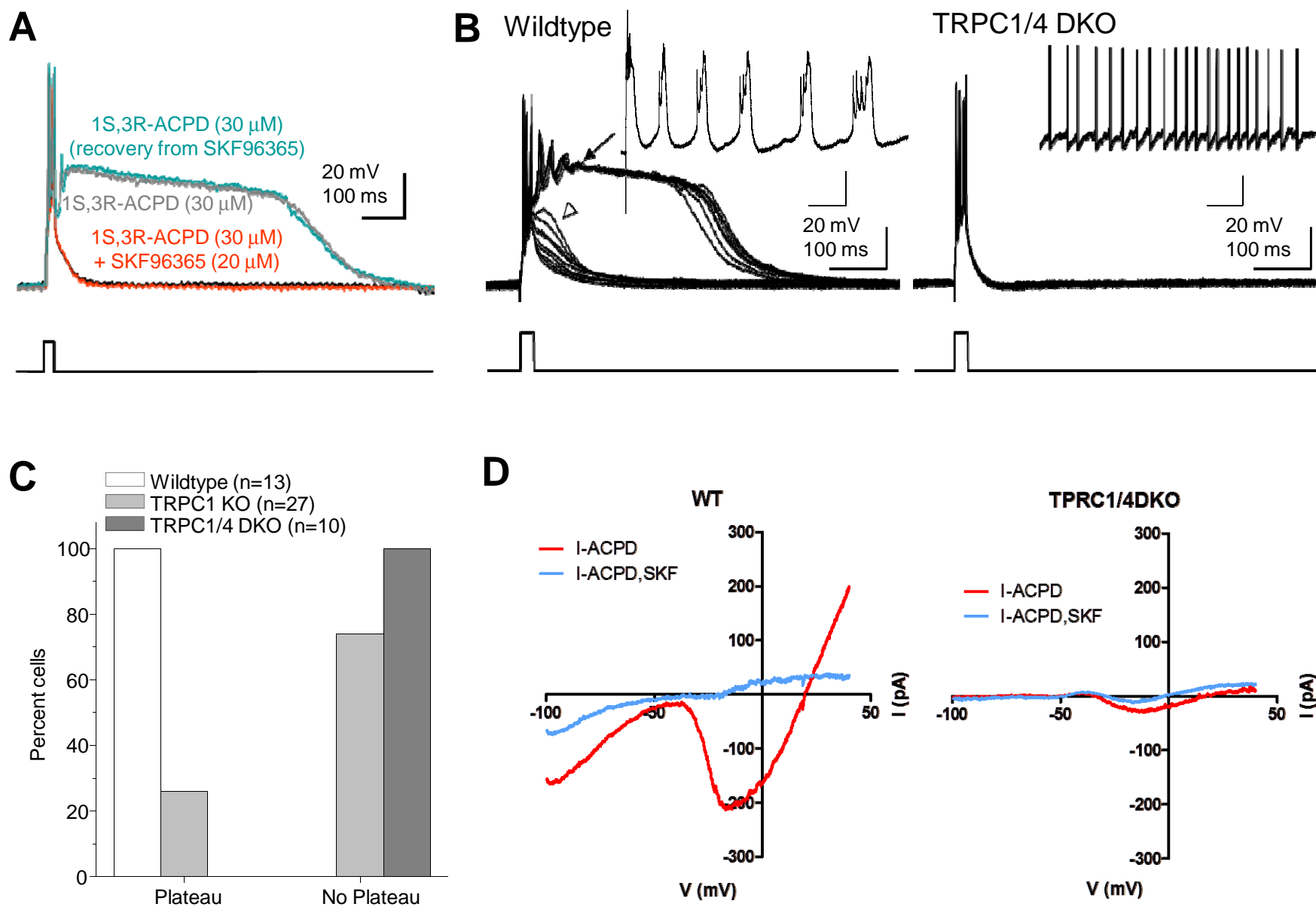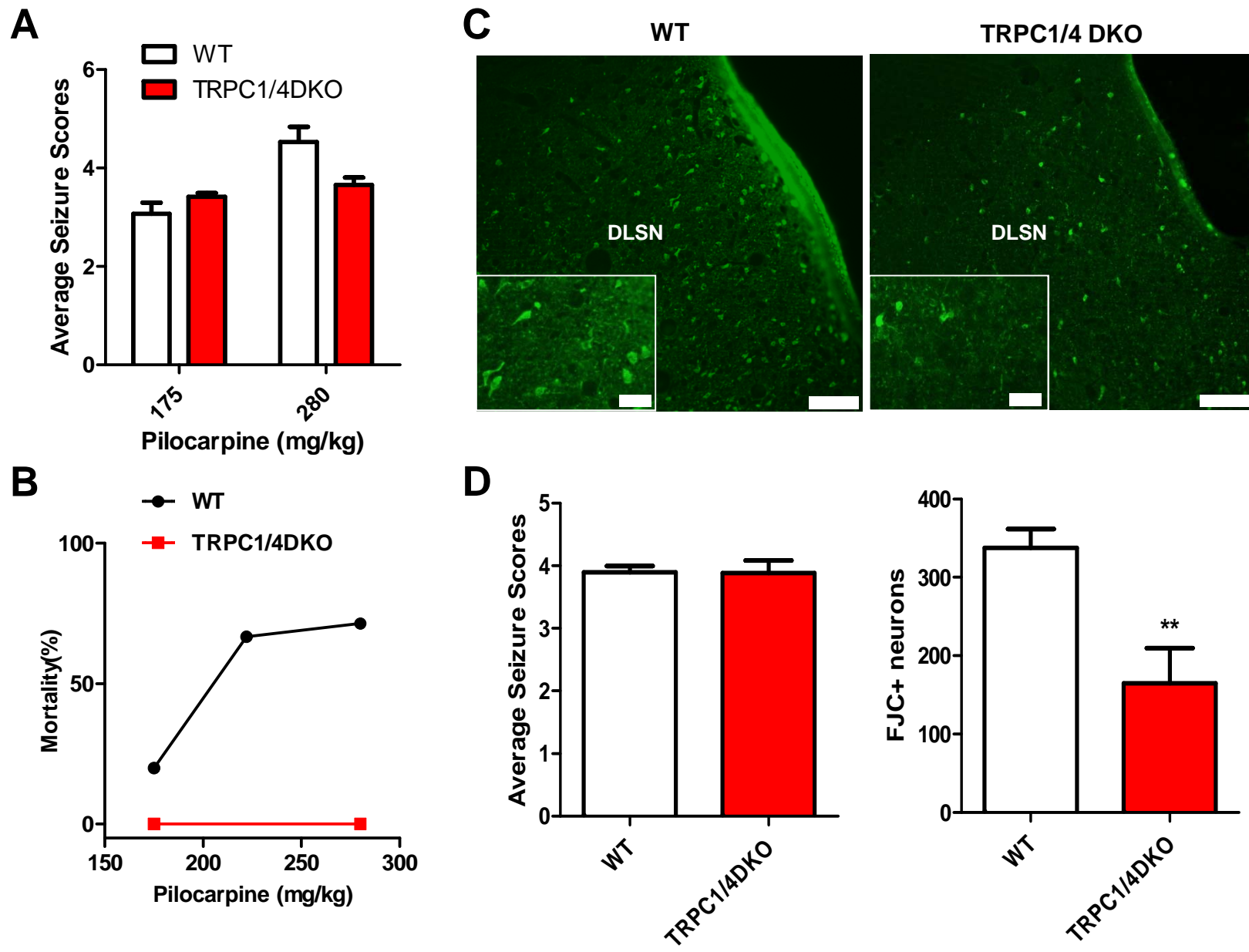
Figure 1

A

Control

1S,3R-ACPD (30 μM)

20 mV
100 ms

20 mV
100 ms

B

1S,3R-ACPD

1S,3R-ACPD
+LY367385

20 mV
200 ms

1S,3R-ACPD

20 mV
100 ms

1S,3R-ACPD
+CPCCOEt

Figure 2

Figure 3

Figure 4

WT, Pilocarpine 175mg/kg

TRPC1/4 KO, Pilocarpine 280mg/kg

Figure 5

Figure 6